Hydrol. Earth Syst. Sci. Discuss., 9, 5515–5529, 2012
www.hydrol-earth-syst-sci-discuss.net/9/5515/2012/
doi:10.5194/hessd-9-5515-2012

Hydrology and Earth System Sciences Discussions

Technical Note: Bias correcting climate model simulated daily temperature extremes with quantile mapping

B. L. Thrasher[1,2], **E. P. Maurer**[3], **C. McKellar**[4], and **P. B. Duffy**[5]

[1]Climate Analytics Group, Palo Alto, CA 94303, USA
[2]Climate Central, Princeton, NJ 08542, USA
[3]Santa Clara University, Civil Engineering Department,
Santa Clara, California, 95053-0563, USA
[4]San Jose State University, Department of Meteorology and Climate Science,
San Jose, CA 95126, USA
[5]Lawrence Livermore National Laboratory, Livermore, CA 94550, USA

Received: 27 March 2012 – Accepted: 11 April 2012 – Published: 25 April 2012

Correspondence to: B. L. Thrasher (bridget@climateanalyticsgroup.org)

Published by Copernicus Publications on behalf of the European Geosciences Union.

Abstract

When applying a quantile-mapping based bias correction to daily temperature extremes simulated by a global climate model (GCM), the transformed values of maximum and minimum temperatures are changed, and the diurnal temperature range (DTR) can become physically unrealistic. While causes are not thoroughly explored, there is a strong relationship between GCM biases in snow albedo feedback during snowmelt and bias correction resulting in unrealistic DTR values. We propose a technique to bias correct DTR, based on comparing observations and GCM historic simulations, and combine that with either bias correcting daily maximum temperatures and calculating daily minimum temperatures or vice versa. By basing the bias correction on a base period of 1961–1980 and validating it during a test period of 1981–1999, we show that bias correcting DTR and maximum daily temperature can produce more accurate estimations of daily temperature extremes while avoiding the pathological cases of unrealistic DTR values.

1 Introduction

While monthly, seasonal, and annual changes in climate have the potential to affect ecosystems and human development (e.g., Fowler and Kilsby, 2003; Palmer and Raisanen, 2002; Schneider et al., 2007), there has been an increasing interest in the effect of shorter-term extreme events (Christensen et al., 2007; IPCC, 2011). These events can cause billions of dollars in damages in hours or days (Bouwer and Vellinga, 2003), and changes in their magnitude and/or frequency are projected to increase the risk of amplified damages in future decades (Easterling et al., 2000).

To assess regional changes in daily extreme rainfall and temperature, global climate model (GCM) output must be downscaled to a more regionally appropriate scale. The many methods to achieve this can be broadly classified as dynamical, which uses a fine-scale climate model to interpolate GCM signals, and statistical, which uses historically derived statistical relationships between GCM-scale and fine-scale features to estimate regional climate (Christensen et al., 2007). In either case, before any downscaled data can be ingested into a model to estimate specific impacts of climate change, some adjustment to account for the GCM biases must be included, since at least some of the bias is systematic, being induced by factors such as inadequate terrain resolution in the GCM (Haerter et al., 2011).

We focus here on a common form of bias correction, namely quantile mapping (Panofsky and Brier, 1968; Wood et al., 2002). The quantile mapping approach has the benefit of accounting for GCM biases in all statistical moments, though, like all statistical downscaling approaches, it is assumed that biases relative to historic observations will be constant during the projections. While this quantile mapping approach has been used extensively for downscaling monthly average precipitation and temperature (Hayhoe et al., 2008; Maurer and Duffy, 2005; Wood et al., 2004), its adaptation to daily data is relatively new (Abatzoglou and Brown, 2011; Maurer et al., 2010). When maximum daily temperature (T_{max}) and minimum daily temperature (T_{min}) are adjusted with quantile-mapping bias correction (hereinafter referred to as BC), the bias correction can modify the diurnal temperature range (DTR) and in some instances can result in the relationship between T_{max} and T_{min} being physically unrealistic (Quintana Seguí et al., 2010). In this study, we compare the different alternatives to (1) minimize the error in the bias corrected T_{max} and T_{min} values, and (2) reduce the frequency of cases where T_{max} and T_{min} are reversed in the BC process. We examine the ability to minimize these instances by instead applying the BC to diurnal temperature range (DTR) and either T_{min} or T_{max}, where the remaining variable is derived by adding or subtracting the DTR as appropriate. In this way GCM-simulated trends in DTR, T_{min} and T_{max} can be retained without the need for ad hoc adjustments.

2 Methods and data

Table 1 lists the 17 GCM simulations from which daily T_{max} and T_{min} values were obtained for the 1961–1999 period. These GCM simulations were archived as part of the World Climate Research Programme's (WCRP's) Coupled Model Intercomparison Project phase 3 (CMIP3) multi-model dataset effort (Meehl et al., 2007). GCM output was interpolated onto a common 2-degree grid to enable intercomparison and summaries across GCMs. For an observational baseline, a 0.5-degree daily global gridded dataset (Adam and Lettenmaier, 2003; Maurer et al., 2009) was aggregated to the same 2-degree grid spacing. DTR was calculated for each day in the 39-yr GCM simulations, as well as for the gridded observations, as the difference between T_{max} and T_{min}.

The BC approach used here is essentially that of Maurer et al. (2010), but rather than being applied to daily average temperatures it is applied to T_{max}, T_{min}, or DTR independently. In summary, the BC uses a base period where both daily observations and daily GCM simulated values are available. For each day of the year, a moving window of ±15 days is used to select all candidate days representative of the date, and all of these candidate days are sorted and ranked to produce for each calendar day two cumulative distribution functions (CDFs), one for observations and one for the GCM. For this study we used 1961–1980 as the base period for which the BC relationships were derived, thus for any calendar date there would be 31 days in the moving window and 20 yr in the base period, resulting in 620 points to define the CDF for each variable. A bias corrected value for a GCM simulated daily value is retrieved by using the CDF for the GCM to determine the quantile associated with the value, and then drawing the observed value from that same day's CDF for the same quantile. For example, a median T_{max} value for 15 February in the GCM output will be transformed into the median T_{max} value in the observations for 15 February, where the median value is that daily value exceeded 50 % of the time in the set of 620 days defining the CDFs for 15 February.

We perform three variations of daily temperature BC:

Case (1) BC performed for T_{max} and T_{min};
Case (2) BC performed for T_{min} and DTR, with T_{max} calculated as T_{min} + DTR;
Case (3) BC performed for T_{max} and DTR, with T_{min} calculated as T_{max} – DTR.

Case 1 is the default case, with shortcomings discussed above. Cases 2 and 3 are evaluated by comparing the root mean square error (RMSE) across all days and grid cells for global land areas, where the RMSE is calculated for the derived variable, i.e. for case 2 RMSE for T_{max} is assessed, and for case 3 RMSE for T_{min} is assessed. The three cases are assessed for the validation period of 1981–1999.

3 Results and discussion

The results for case 1 are shown in Fig. 1. Despite the wide variability in the number of cases where $T_{min} > T_{max}$ after BC of the GCM output, Fig. 1 shows, for extreme high and low cases, that these tend to occur predominantly at high latitudes (and this is generally the case for all of the GCM runs used in this study). For these high latitude regions the GCMs have biases in mean and/or variability that tend to produce more occurrences of $T_{min} > T_{max}$ when adjusted through BC. For most GCM runs the greatest number of cases occurs in March–May, or during the Northern Hemisphere snowmelt season. Hall and Qu (2006) identified GCM biases in the representation of melt season snow albedo in the Northern Hemisphere as a major factor in the variability in GCM-simulated climate sensitivity. While a thorough investigation of this is ongoing, the GCM error in snow albedo feedback (from the abscissa of Fig. 3 in Hall and Qu) and the frequency of $T_{min} > T_{max}$ occurrences in this study are highly significantly correlated (Pearson r^2 = 0.87; Fig. 2), illustrating a strong relation between GCM biases in snow albedo and the biases in daily surface air temperatures that cause more $T_{min} > T_{max}$ occurrences during BC, though causality has not yet been determined. It should be noted that even in the extreme case over Eastern Europe for the worst case of the GCMs used here, fewer than 400 occurrences are observed in the 19 yr validation period, indicating less than

6 % of days having $T_{\mathrm{min}} > T_{\mathrm{max}}$, with most of global land areas and GCM runs exhibiting far less than this. On average for all GCM runs $T_{\mathrm{min}} > T_{\mathrm{max}}$ occurs approximately 0.25 % of the time.

The two approaches conducted in this study to remedy the occurrence of $T_{\mathrm{min}} > T_{\mathrm{max}}$ following the BC process, cases 2 and 3, are compared to determine the preferable alternative. Figure 3 shows the results for case 2, where the "original T_{max}" RMSE refers to T_{max} produced as in case 1, and the "derived T_{max}" being that calculated as described above for case 2. The increased RMSE shown in Fig. 3 shows that for all GCM simulations this approach, while eliminating occurrences of $T_{\mathrm{min}} > T_{\mathrm{max}}$, deteriorates the estimation of T_{max} in the BC process.

Figure 4 shows similar results to Fig. 3 but for case 3. In this alternative, "original T_{min}" refers to the BC T_{min} as in case 1, and "derived T_{min}" is that calculated according to the description of case 3 above. In contrast to case 2, the T_{min} values derived in case 3 show reduced RMSE for 12 of the 17 GCM simulations, indicating that this alternative not only removes the possibility of $T_{\mathrm{min}} > T_{\mathrm{max}}$ in the BC process, but results in an improved estimation of T_{min} on average.

Finally, while case 3 appears the best solution of the alternatives assessed in this study, since applying BC to DTR is a new application, we verified that DTR is not degraded in the BC process (Fig. 5). The RMSE for DTR relative to observations (for the 1981–1999 validation period) is reduced on average 28 % after BC.

4 Conclusions

We evaluated the potential to improve the quantile mapping bias correction approach when applied to daily GCM output of maximum and minimum temperatures. A direct bias correction of both T_{max} and T_{min} results in some cases where the unrealistic occurrence of $T_{\mathrm{min}} > T_{\mathrm{max}}$ appears. To remedy this, we first derive the diurnal temperature range for each day, and then apply the bias correction to DTR and either T_{max} or T_{min}, calculating the remaining variable.

We find that bias correcting daily DTR and T_{max}, and calculating T_{min} as T_{max} – DTR eliminates the occurrence of $T_{min} > T_{max}$ and in general improves the estimation of T_{min} compared to bias correcting T_{min} directly. This approach will be further assessed and implemented in future applications of quantile mapping bias correction of daily GCM temperature output.

Acknowledgements. Funding for this work was provided by the US Army Corps of Engineers under grant W912HQ-IWR-CLIMATE. We acknowledge the modeling groups, the Program for Climate Model Diagnosis and Intercomparison (PCMDI) and the WCRP's Working Group on Coupled Modelling (WGCM) for their roles in making available the WCRP CMIP3 multi-model dataset. Support of this dataset is provided by the Office of Science, US Department of Energy.

References

Abatzoglou, J. T. and Brown, T. J.: A comparison of statistical downscaling methods suited for wildfire applications, Int. J. Climatol., doi:10.1002/joc.2312, in press, 2011.

Adam, J. C. and Lettenmaier, D. P.: Adjustment of global gridded precipitation for systematic bias, J. Geophys Res., 108, 1–14, 2003.

Bouwer, L. and Vellinga, P.: Changing climate and increasing costs – implications for liability and insurance climatic change: implications for the hydrological cycle and for water management, in: Advances in Global Change Research, edited by: Beniston, M., Springer Netherlands, 429–444, 2003.

Christensen, J. H., Hewitson, B., Busuioc, A., Chen, A., Gao, X., Held, I., Jones, R., Kolli, R. K., Kwon, W.-T., Laprise, R., Magaña Rueda, V., Mearns, L., Menéndez, C. G., Räisänen, J., Rinke, A., Sarr, A., and Whetton, P.: Regional climate projections, in: Climate Change 2007: The Physical Science Basis, Contribution of Working Group I to the Fourth Assessment Report of the Intergovernmental Panel on Climate Change, edited by: Solomon, S., Qin, D., Manning, M., Chen, Z., Marquis, M., Averyt, K. B., Tignor, M., and Miller, H. L., Cambridge University Press, Cambridge, New York, 2007.

Easterling, D. R., Meehl, G. A., Parmesan, C., Changnon, S. A., Karl, T. R., and Mearns, L. O.: Climate extremes: observations, modeling, and impacts, Science, 289, 2068–2074, 2000.

Fowler, H. J. and Kilsby, C. G.: Implications of changes in seasonal and annual extreme rainfall, Geophys. Res. Lett., 30, 1720, doi:10.1029/2003gl017327, 2003.

Haerter, J. O., Hagemann, S., Moseley, C., and Piani, C.: Climate model bias correction and the role of timescales, Hydrol. Earth Syst. Sci., 15, 1065–1079, doi:10.5194/hess-15-1065-2011, 2011.

Hall, A. and Qu, X.: Using the current seasonal cycle to constrain snow albedo feedback in future climate change, Geophys. Res. Lett., 33, L03502, doi:10.1029/2005gl025127, 2006.

Hayhoe, K., Wake, C., Anderson, B., Liang, X.-Z., Maurer, E., Zhu, J., Bradbury, J., DeGaetano, A., Stoner, A., and Wuebbles, D.: Regional climate change projections for the Northeast USA, Mitigat. Adapt. Strat. Global Change, 13, 425–436, 10.1007/s11027-007-9133–2, 2008.

Field, C. B., Barros, V., Stocker, T. F., Qin, D., Dokken, D., Ebi, K. L., Mastrandrea, M. D., Mach, K. J., Plattner, G.-K., Allen, S. K., Tignor, M., and Midgley, P. M. (Eds.): IPCC: Intergovernmental Panel on Climate Change Special Report on Managing the Risks of Extreme Events and Disasters to Advance Climate Change Adaptation, Summary for Policymakers, Cambridge University Press, Cambridge, 2011.

Maurer, E. P. and Duffy, P. B.: Uncertainty in projections of streamflow changes due to climate change in California, Geophys. Res. Lett., 32, L03704, doi:10.1029/2004GL021462, 2005.

Maurer, E. P., Adam, J. C., and Wood, A. W.: Climate model based consensus on the hydrologic impacts of climate change to the Rio Lempa basin of Central America, Hydrol. Earth Syst. Sci., 13, 183–194, doi:10.5194/hess-13-183-2009, 2009.

Maurer, E. P., Hidalgo, H. G., Das, T., Dettinger, M. D., and Cayan, D. R.: The utility of daily large-scale climate data in the assessment of climate change impacts on daily streamflow in California, Hydrol. Earth Syst. Sci., 14, 1125–1138, doi:10.5194/hess-14-1125-2010, 2010.

Meehl, G. A., Covey, C., Delworth, T., Latif, M., McAvaney, B., Mitchell, J. F. B., Stouffer, R. J., and Taylor, K. E.: The WCRP CMIP3 multimodel dataset: A new era in climate change research, B. Am. Meteorol. Soc., 88, 1383–1394, 2007.

Palmer, T. N. and Raisanen, J.: Quantifying the risk of extreme seasonal precipitation events in a changing climate, Nature, 415, 512–514, 2002.

Panofsky, H. A. and Brier, G. W.: Some Applications of Statistics to Meteorology, The Pennsylvania State University, University Park, 224 pp., 1968.

Quintana Seguí, P., Ribes, A., Martin, E., Habets, F., and Boé, J.: Comparison of three downscaling methods in simulating the impact of climate change on the hydrology of Mediterranean basins, J. Hydrol., 383, 111–124, 2010.

Schneider, S. H., Semenov, S., Patwardhan, A., Burton, I., Magadza, C. H. D., Oppenheimer, M., Pittock, A. B., Rahman, A., Smith, J. B., Suarez, A., and Yamin, F.: Assessing key vulnerabilities and the risk from climate change, in: Climate Change 2007: Impacts, Adaptation and Vulnerability. Contribution of Working Group II to the Fourth Assessment Report of the Intergovernmental Panel on Climate Change, edited by: Parry, M. L., Canziani, O. F., Palutikof, J. P., van der Linden, P. J., and Hanson, C. E., Cambridge University Press, Cambridge, 779–810, 2007.

Wood, A. W., Maurer, E. P., Kumar, A., and Lettenmaier, D. P.: Long-range experimental hydrologic forecasting for the Eastern United States, J. Geophys Res., 107, 4429, doi:10.1029/2001JD000659, 2002.

Wood, A. W., Leung, L. R., Sridhar, V., and Lettenmaier, D. P.: Hydrologic implications of dynamical and statistical approaches to downscaling climate model outputs, Climatic Change, 62, 189–216, 2004.

Table 1. GCMs and run numbers included in this study.

	Simulation
1	CCCMA-CGCM3-1: Run 1
2	CCCMA-CGCM3-1: Run 2
3	CCCMA-CGCM3-1: Run 3
4	CNRM-CM3
5	GFDL-CM2-0
6	GFDL-CM2-1
7	IPSL-CM4
8	MIROC3-2-MEDRES: Run 1
9	MIROC3-2-MEDRES: Run 2
10	MIUB-ECHO-G: Run 1
11	MIUB-ECHO-G: Run 2
12	MIUB-ECHO-G: Run 3
13	MPI-ECHAM5
14	MRI-CGCM2.3.2A: Run 1
15	MRI-CGCM2.3.2A: Run 2
16	MRI-CGCM2.3.2A: Run 3
17	MRI-CGCM2.3.2A: Run 4

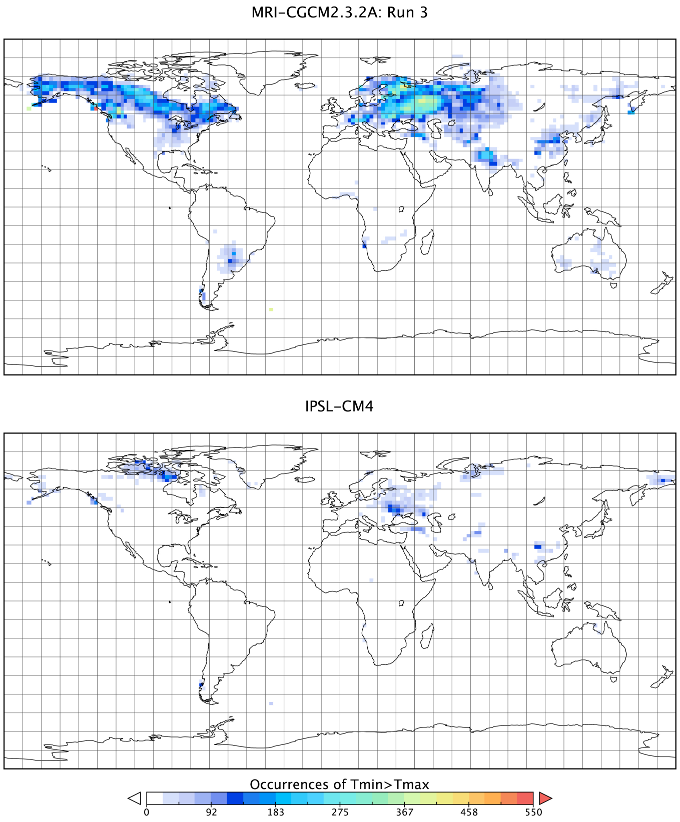

Fig. 1. For case 1, the total number of occurrences for the validation period of 1981–1999 where $T_{\text{min}} > T_{\text{max}}$ after BC. Results for two GCM simulations are shown: a high number of occurrences (upper panel) and a low number of occurrences (lower panel).

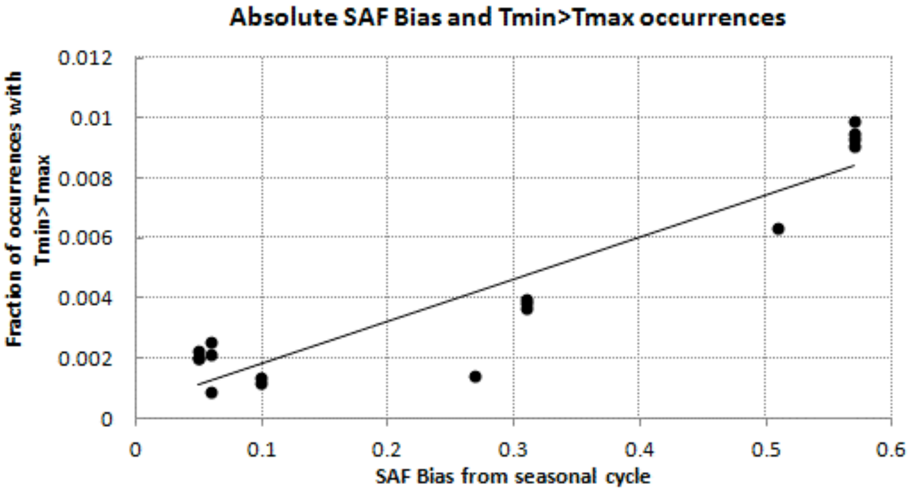

Fig. 2. Fraction of occurrences across all (land area) GCM grid cells and all March–May days in the validation period of 1981–1999 versus the snow albedo feedback error, calculated from Hall and Qu (2006) based on GCM simulated seasonal cycle between Aril and May.

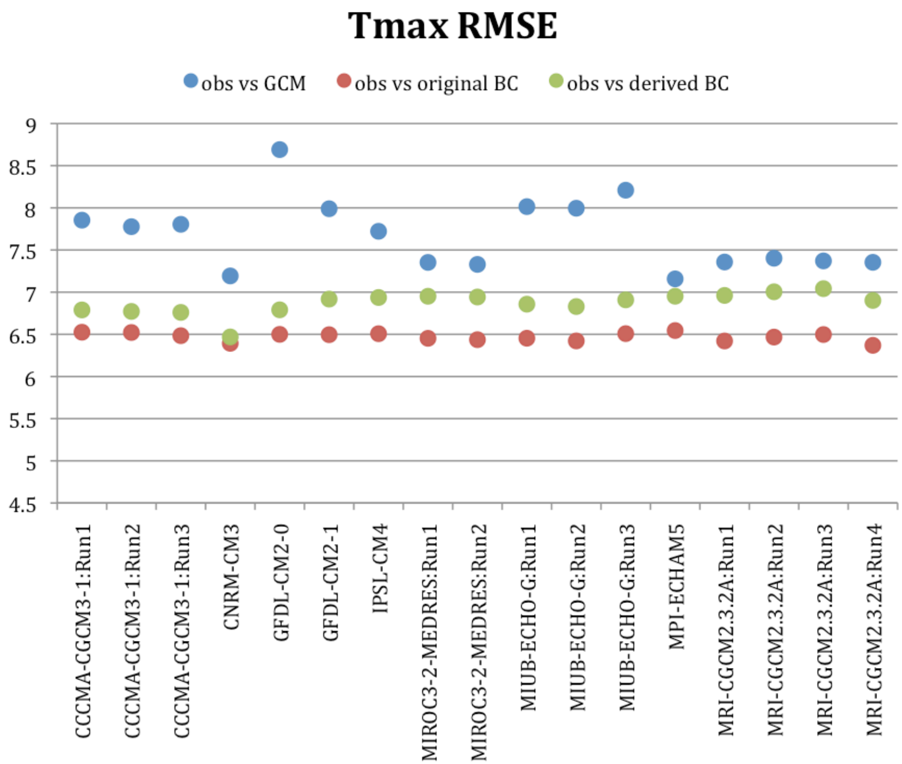

Fig. 3. The RMSE (°C) between gridded observations and three versions of T_{max} for 17 GCM simulations: regridded daily GCM T_{max} (blue), bias corrected daily GCM T_{max} (red), and daily T_{max} derived from bias corrected DTR and T_{min} (green, case 2).

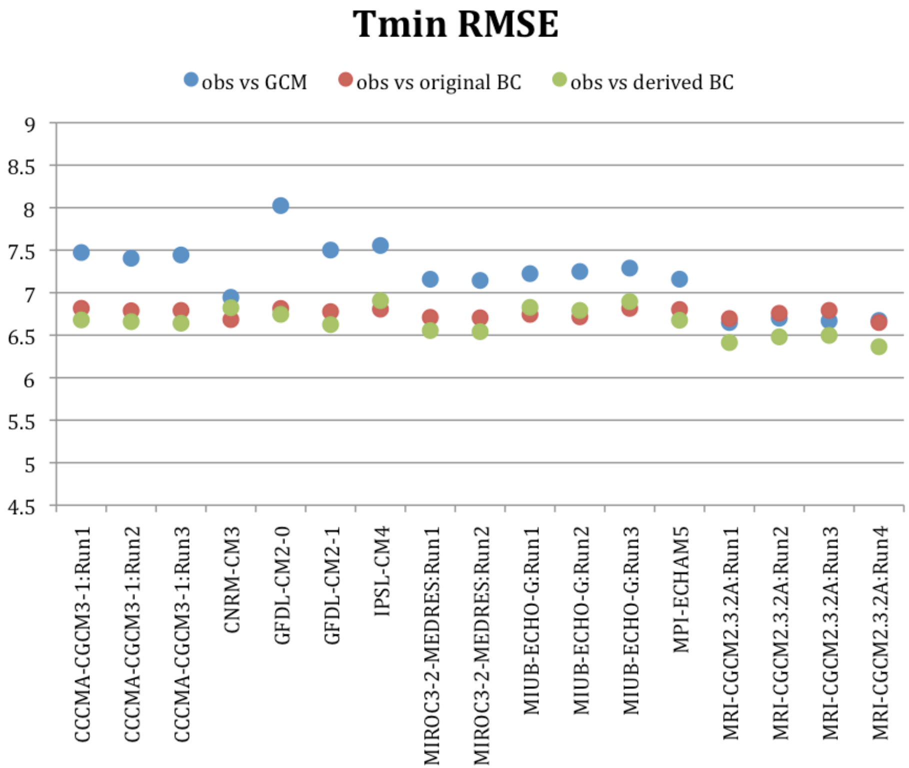

Fig. 4. The RMSE (°C) between gridded observations and three versions of T_{min} for 17 GCM simulations: regridded daily GCM T_{min} (blue), bias corrected daily GCM T_{min} (red), and daily T_{min} derived from bias corrected DTR and T_{max} (green, case 3).

Title Page
Abstract | Introduction
Conclusions | References
Tables | Figures
◀I | ▶I
◀ | ▶
Back | Close
Full Screen / Esc
Printer-friendly Version
Interactive Discussion

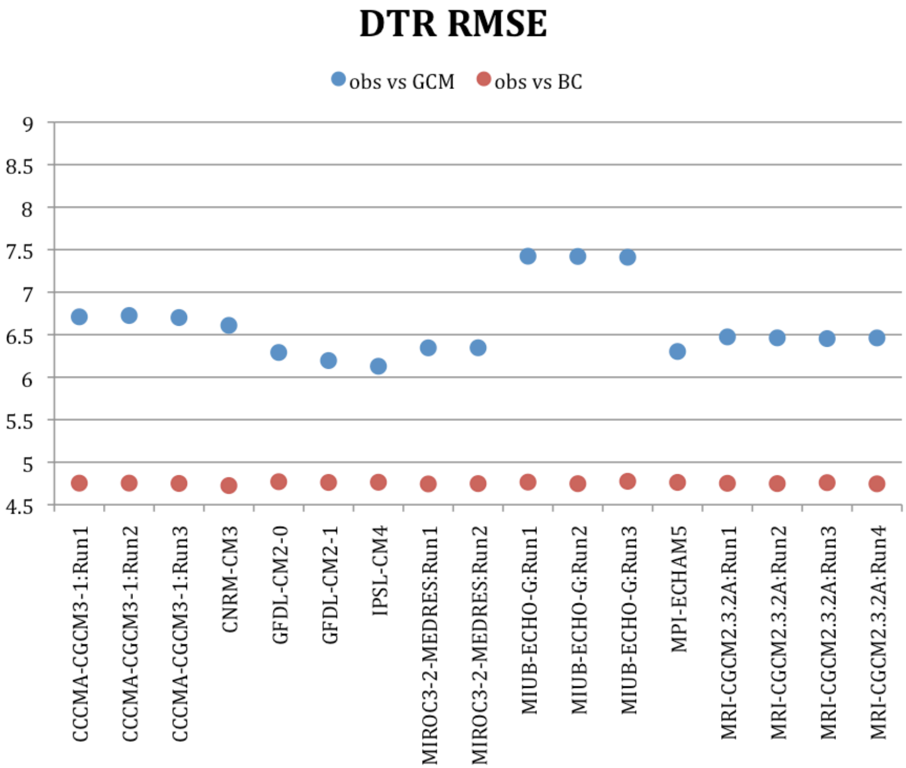

Fig. 5. RMSE (˚C) between gridded observations and two versions of DTR for 17 GCM simulations: regridded daily GCM DTR (blue) and bias corrected daily GCM DTR (red).